NASA Technical Memorandum 83279

NASA-TM-83279 19820015365

TRANSONIC FLUTTER STUDY OF A WIND-TUNNEL MODEL OF A SUPERCRITICAL WING WITH/WITHOUT WINGLET

Charles L. Ruhlin, Frank J. Rauch, Jr., and Catherine Waters

March 1982

National Aeronautics and Space Administration

Langley Research Center
Hampton, Virginia 23665

TRANSONIC FLUTTER STUDY OF A WIND-TUNNEL MODEL OF A SUPERCRITICAL WING WITH/WITHOUT WINGLET

Charles L. Ruhlin*
NASA Langley Research Center, Hampton, Va.

Frank J. Rauch, Jr.,** and Catherine Waters**
Grumman Aerospace Corporation, Bethpage, N.Y.

Abstract

The scaled flutter model was a 1/6.5-size, semispan version of a supercritical wing (SCW) proposed for an executive-jet-transport airplane. The model was tested cantilever-mounted in the Langley Transonic Dynamics Tunnel with a normal wingtip, a wingtip with winglet, and a normal wingtip ballasted to simulate the winglet mass properties. Flutter and aerodynamic data were acquired at Mach numbers (M) from 0.6 to 0.95. The measured transonic flutter speed boundary for each wingtip configuration had roughly the same shape with a minimum flutter speed near M = 0.82. The winglet addition and wingtip mass ballast decreased the wing flutter speed by about 7 and 5 percent, respectively; thus, the winglet effect on flutter was more a mass effect than an aerodynamic effect. Flutter characteristics calculated using a doublet-lattice analysis (which included interference effects) were in good agreement with the experimental results up to M = 0.82. Comparisons of measured static aerodynamic data with predicted data indicated that the model was aerodynamically representative of the airplane SCW.

Nomenclature

C_D	drag coefficient at cruise lift
C_L	wing lift coefficient
C_{L_α}	wing lift-curve slope, 1/deg
C_p	static pressure coefficient, $(= (p-p_s)/q)$
f	frequency, Hz
g	structural damping coefficient
M	Mach number
p	local static pressure
p_s	free-stream static pressure
q	dynamic pressure
t/c	airfoil maximum thickness to chord ratio
V_F/V_{REF}	normalized equivalent flutter speed $(= \sqrt{q_F/q_{REF}})$
α_o	angle of attack at zero lift, deg

I. Introduction

The aerodynamic efficiency of aircraft can be improved appreciably by the use of wings with supercritical airfoils and/or by the addition of wingtip mounted winglets.[1-4] Information on the flutter aspects of these configurations is limited, but the results of available studies[5-11] have shown that the use of either a supercritical airfoil or winglet can reduce appreciably the flutter speed of a wing. Further, these studies indicate that the flutter characteristics of supercritical wings and, in some instances of wings with winglets, may not be predicted accurately by conventional analytical methods. Because supercritical wings and wings with winglets are in use or being considered for use on high-speed executive jet transports, the present study was undertaken to provide guidance for the flutter design of such aircraft and to enlarge the flutter data base on supercritical wings and winglets.

The specific objectives of the present study were (1) to determine experimentally the effect of a winglet on the transonic flutter characteristics of a realistic supercritical wing, (2) to correlate these experimental results with analyses, (3) to explore for angle-of-attack induced flutter, and (4) to examine effects of elastic deformations on some aerodynamic characteristics of this supercritical wing. The model used in this study was a 1/6.5-size, dynamically and elastically scaled semispan version of a supercritical wing proposed for an executive jet transport. This airplane had a cruise Mach number of 0.82 and its wing was designed to carry a winglet for increased aerodynamic performance. To separate the mass effect from the aerodynamic effect of the winglet, the model was tested with three interchangeable wingtips: a normal tip, a tip with a winglet, and a normally shaped tip that was mass ballasted to simulate the winglet mass and pitch inertial properties. The model was tested cantilever-mounted on a five-component aerodynamic force balance attached to the sidewall of the Langley Transonic Dynamics Tunnel as shown in Figure 1. The model was equipped with orifices at the 0.30 semispan station to measure the chordwise static pressure distribution.

Pretest flutter analyses were made for each wingtip configuration using doublet lattice unsteady aerodynamics which included wing/winglet interference effects.[12] Wing static pressure distributions at two tunnel test conditions were calculated using a Jameson full potential aerodynamic code (FL022) for use as part of the model aerodynamic verification.[13] This code cannot model fuselage effects.

The tests covered a Mach number range from about 0.6 to 0.95 and were conducted in three phases. First, static aerodynamic data were measured at near scaled airplane cruise conditions to verify that the flutter model was aerodynamically representative of the airplane supercritical wing (SCW) both with and without winglet.

*Aero-Space Technologist, Configuration Aeroelasticity Branch, Loads and Aeroelasticity Division. Member AIAA.

**Senior Engineer, Loads and Dynamics Section, Engineering Department. Member AIAA.

Secondly, tests were made to explore for angle-of-attack induced flutter within the scaled airplane flight envelope. Limited static aerodynamic data were also acquired during these tests.

During the angle-of-attack tests, the advantages of lowering the wing flutter dynamic pressure level from that predicted by analysis became obvious. Primarily, it was felt that flutter data for a SCW would be more meaningful if it were obtained with the wing in a lifting condition. Hence, investigation of a flutter boundary closer to the design flight envelope was desirable since the aeroelastic deformations in this regime correspond to realistic design constraints. Secondly, because of the extreme aeroelastic deformations expected at the predicted high flutter dynamic pressure levels, simply trimming the model becomes difficult within the strength limitations of the model, and the model survival at flutter appeared problematical at best. To reduce the flutter dynamic pressures to reasonably low levels, mass ballast was added to the wing trailing edge and enclosed within flap track fairings which were present on the airplane but had not previously been used on the model. Although the actual mass that was added exceeded the scaled total mass of the flap track fairings, flutter analyses indicated that the flutter mechanism remained essentially the same. The angle-of-attack induced flutter search was continued with this configuration.

In the third test phase, the transonic flutter characteristics of the wing (with ballasted flap track fairings) with each wingtip were determined. The model was destroyed during flutter but not before a flutter boundary for each configuration had been reasonably well defined. For comparison with the experimental results, flutter analyses were made for each wingtip configuration.

Presented herein are the significant results of this study. Some detailed test and analytical results, including model physical properties in sufficient detail for independent analysis, are reported in reference 14.

II. Model

In the present paper, the clean wing is defined as the wing without flap track fairings. Some scaling ratios for the clean wing model and model dimensions are presented in Figures 2 and 3. The scaled airplane flight envelope for the clean wing model in the wind tunnel is included in Figure 2. The exposed semispan wing had an aspect ratio of 3.7 and a 27° sweepback angle of the quarter-chord line. The winglet area was about 1/25 that of the exposed wing semispan. It should be noted that the mass scaling ratio and scaled flight envelope (Fig. 2) do not apply to the wing with the ballasted flap track fairings because the mass of the ballast weights and fairings that was actually used was much greater than the scaled airplane values.

The semispan model was cantilever-mounted on an aerodynamic force balance that was attached to the tunnel sidewall turntable. Enclosing the balance and wing root was a half-fuselage shaped aerodynamic fairing that was attached to the turntable separate from the balance (Fig. 1). The fairing allowed the wing to be tested outside the boundary layer of the tunnel wall.

Two different transition strips were used on the model. For tests near the scaled cruise dynamic pressure of 30 psf, the transition strip was located on the upper and lower wing surface along the entire semispan at the 40-percent chord line. For tests at all higher dynamic pressures, the transition strip over the span outboard of the wing edge break was moved forward to about the 10-percent chord line. Although this high-q transition strip was designed to provide proper flow transition at $M = 0.82$ and $q = 90$ psf, it was considered applicable at higher dynamic pressures and reasonably adequate at much lower dynamic pressures.

Construction

The basic structure of the model wing consisted of front and rear fiberglass spars and fiberglass ribs to which were bonded fiberglass cover skins. Foam plastic panels about 0.5 inch in thickness were bonded to the interior sides of the skins between the ribs and spars to prevent local buckling. The three interchangeable wingtips were constructed basically the same as the wing. Each wingtip was mounted to the wing through attachment tabs that extended outboard from the main wing structure; the wingtip-to-wing section joint was covered with thin paper tape to form an aerodynamically smooth surface.

For the latter part of the tests, five aft-mounted flap track aerodynamic fairings were attached to the wing (Figs. 1 and 3). The fairings were hollow balsa shells that were bonded to the wing surfaces. Ballast weights were attached to the wing and enclosed within the three outermost fairings.

Instrumentation

Strain gages for measuring the bending and torsional moments were located at three different wing spanwise stations and on the winglet root. To measure a chordwise static pressure distribution, 20 pressure orifices were located at the 0.30 semispan station (the wing edge break) with 13 and 7 taps on the upper and lower wing surface, respectively. Tubes from these orifices ran to a scanivalve located in the fuselage.

Ten "bending beams" were distributed along the span of each wing spar. These bending beams were thin, narrow metallic beams about 1 inch long that were equipped with strain gages. They were fastened to the mid-chord of the spars so that the wing spar bending slopes at each beam station could be measured. The intent was that by integration of the measured spar slopes the wing bending and twist distribution could be determined. This system was to some degree successful. Some results obtained with this system during the present tests have been reported[15] and therefore will not be discussed in this paper.

Physical Properties

For analysis purposes, the clean wing was divided into nine spanwise panels (boundaries

oriented streamwise) and each wingtip was considered separately as a part of the most outboard wing panel. The mass and inertial properties of the model wing panels were determined by scaling the airplane design values. These scaled panel properties were adjusted for best agreement with those measured for the structural components during construction and for the completed model; the adjusted panel properties were used in the vibration and flutter analyses. For the vibration analyses of the wing with flap track fairings, each fairing and, where present, its enclosed ballast weight was treated as a single mass (separate from the wing panel) having a node point at its center of gravity.

The measured mass and inertial properties of the three wingtips are given in Table I. The ballasted tip matches the mass properties of the winglet tip fairly well except for the spanwise center-of-gravity (c.g.) location and roll inertia which were considered of lesser importance to flutter. The total mass of the clean wing with the normal wingtip was 15.3 lbm. The mass of the winglet alone was 0.234 lbm. The total mass of the flap track fairings and enclosed ballast weights added to the model was 4.6 lbm, which was about 20 times greater than the scaled value for the airplane flap track mechanisms and structures of 0.235 lbm. It was realized that the mass scaling of the model to the airplane was radically altered when the ballasted flap track fairings were added to the wing. Nevertheless, this effect was considered outweighed by the advantages resulting from lowering the flutter dynamic pressures closer to the clean-wing flight envelope. As mentioned before, flutter analyses indicated the flutter mechanism was basically the same for both the clean wing and wing with flap track fairings.

Bending and twist slopes were measured along and about the 40-percent chord line (elastic axis) from which bending (EI) and torsional (GJ) stiffness distributions were determined. From these stiffnesses, an 18 by 18 flexibility influence coefficient matrix for bending and twist along the elastic axis was derived. In general, both the distributions and levels of mass and stiffness of the clean-wing model were in good agreement with scaled airplane values.

III. Vibration Characteristics

Some measured and calculated vibration characteristics of the various model configurations are presented in Figures 4 and 5. In these figures, only a single node line pattern is shown for the modes which were both calculated and measured because the nodal patterns were essentially identical. Although up to six vibration modes were measured and calculated, only data for the first four vibration modes are presented because they were the most important to flutter. For the vibration measurements, the model was mounted to the aerodynamic force balance which was bolted to either a rigid backstop or the tunnel turntable. The different mounting methods had no appreciable effect on the model vibration data measured for one check case.

With the winglet tip section clamped so that the winglet was essentially cantilevered, the winglet fundamental (bending) frequency was measured at 78 Hz, a considerably higher frequency than those for the wing modes important to flutter (Figs. 4 and 5). Therefore, winglet flexibility was not considered to be a significant factor in the present flutter study.

Clean Wing

For the clean wing, vibration surveys, which included mode shape measurements, were made for the three wingtip configurations (Fig. 4). The addition of the winglet decreased the wing (normal tip) frequencies by about 6 to 10 percent for the bending modes and by about 13 percent for the torsional (58 Hz) mode. The modal characteristics of the winglet tip configuration were matched fairly well by the ballasted tip configuration.

The vibration characteristics of the ballasted tip configuration were calculated for comparison with the experimental data. The vibration analysis employed the measured flexibility influence coefficients and the adjusted panel mass properties. The calculated vibration mode frequencies varied from about -6 to +3 percent of the corresponding measured values (Fig. 4). Overall, the analytical results were in good agreement with the experimental data. It was concluded that the panel mass distributions could be used with confidence in the vibration and flutter analyses. Generalized masses were calculated for each wingtip configuration using the measured mode shapes and panel mass properties. The off-diagonal terms in the generalized masses were found to be relatively small (indicating the measured mode shapes were reasonably orthogonal) and were therefore neglected in the flutter analyses.

Wing with Flap Track Fairings

For the wing with the flap track fairings, the vibration characteristics of the wing with each wingtip configuration were calculated (Fig. 5). These results were obtained by a mass coupling of the flap track fairings with the measured vibration modal data for the clean wing with the corresponding wingtip configuration. A cursory vibration survey of the winglet configuration was made that included a check of the mode shape displacement at selected wing locations. The measured data agreed reasonably well with the calculated results (Fig. 5).

The addition of the ballasted flap track fairings to the wing sizably reduced the vibration-mode frequencies for all three tip configurations, although the general character and order of the modes were retained (see Figs. 4 and 5). However, the addition of the winglet only slightly reduced the wing torsional frequency from 39.61 to 39.03 Hz (Figs. 5(a) and (b)), as compared to much greater reductions for the clean-wing case. This is probably due to the fact that the winglet was now a much smaller part of the total wing mass moment of inertia and also that the addition of the flap tracks had moved the wing torsional node line rearward and closer to the winglet center-of-gravity.

Again, the ballasted-tip modal data agree overall reasonably well with the corresponding winglet-tip data (Figs. 5(b) and (c)).

IV. Wind-Tunnel Test Procedure

The model tests were conducted using Freon* in the Langley Transonic Dynamics Tunnel (TDT) at Mach numbers up to about 0.95. The model was tested cantilever-mounted on a five-component aerodynamic balance attached to a sidewall turntable (Fig. 1). The turntable was remotely controlled and could rotate the model and fuselage body through a wide angle-of-attack range. The balance measured normal and axial forces and pitch, roll, and yaw moments.

Electrical output signals from the balance, scanivalve, and model strain gages were circuited to the TDT Data Acquisition System (DAS).[16] On command, the DAS provided a printout of the reduced test data and tunnel parameters. It also provided graphic displays to the test operator of plots of selected aerodynamic force vs angle-of-attack data, chordwise static pressure distribution, and wing bending and twist deflections (determined from integrating the wing beam slope measurements).

During the test, the lift and vibrations of the wing and winglet (as measured by the surface strain gages) were continuously monitored on recording galvanometer strip charts. Also monitored was a continuously updated frequency spectrum of the model response that was obtained using a real-time frequency analyzer. When aerodynamic data were recorded, the twist angle and vertical displacement of the model wingtip were measured visually with a cathetometer that was aimed through the test-section viewing windows.

Generally, the tunnel was operated at a nearly constant stagnation pressure while M and consequently q were increased until the maximum test M limit was reached or flutter occurred. Aerodynamic data were acquired at dwell points of constant M and q. The M sweeps were repeated with the stagnation pressure incrementally increased in steps from an initial low value until the desired data had been obtained. Visual records at flutter were obtained using high-speed motion picture cameras. A continuous visual record of the model behavior during the test was obtained using two closed-circuit TV cameras.

V. Aerodynamic Verification Results

The purpose of the aerodynamic verification tests was to verify that the present aeroelastic model was aerodynamically representative of the airplane SCW both with and without winglet. Only clean-wing configurations were used in these tests. The ballasted-tip configuration, which had the conventional wingtip geometry, was tested as the basic wing configuration.

First, by using darkened oil film, flow patterns were observed for the ballasted-tip configuration at the scaled cruise condition ($M = 0.82$, $q = 30$ psf). Aerodynamic data were then measured for the winglet and ballasted-tip configuration at the scaled cruise q over a Mach number range from about 0.6 to 0.85, and these results are presented in Figure 6. It can be seen (fig. 6(b)) that the addition of the winglet decreased the drag coefficient (measured at a scaled cruise lift) over the test Mach number range and increased the Mach number of the compressibility drag-break. Also, the wing with winglet had about a 5 percent higher lift curve slope than the basic wing (Fig. 6(a)). Overall, the flow patterns and aerodynamic data obtained with the flutter model were consistent with comparable test results (unpublished) obtained with rigid aerodynamic models.

Static pressures were measured on the ballasted-tip configuration at the scaled cruise condition and at a higher q, off-design condition ($M = 0.82$, $q = 150$ psf) where the wing aeroelastic deformation would be representative of that near flutter. The chordwise C_p distributions at the 0.30 semispan station measured for the scaled level flight (1 g) lift condition are given in Figure 7. Included are calculated data for both q levels and experimental data (unpublished) from a rigid aerodynamic model test at a representative cruise condition. The pressures were calculated using a Jameson full potential aerodynamic code (FL022) and the measured influence coefficients in an iterative load-deformation procedure. Details of this procedure and additional analytical results are presented in reference 13.

At the cruise condition, the three pressure distributions are in good agreement with the possible exception of the aft section of the lower surface. These differences between the test and analytical results are possibly due to the inability of the potential flow code to model viscous effects. These effects are very important in the aft, cove region of the lower surface of a supercritical airfoil. At the high-q condition, the pressure distribution shapes are quite similar. Again, the most notable difference occurs over the aft portion of the lower surface. It was noted in reference 13 that at the high q condition, the bending and twist deflection measured at the model wingtip was significantly less than those calculated. This discrepancy was attributed at least in part to a separation of the flow over the wing midspan that caused less actual deformation of the wing than was predicted by analysis. It also appears that increasing q results in wing deformations that cause the pressure distribution for a SCW to be distorted considerably more than would be expected for a conventional wing. This could result in shifts of the shock locations and, therefore, in the aerodynamic forces important to flutter.

Based on the oil flow observations, the aerodynamic data trends, and the static pressures comparisons, it was concluded that the flutter model was a very good aerodynamic representation of the airplane SCW.

*Freon: Registered trademark of E. E. duPont de Nemour and Co., Inc.

VI. Angle-of-Attack Test Results

A limited search for possible angle-of-attack induced flutter was made within the scaled flight envelope. Typically, initial low-q tests were made using the clean wing, and later, high-q tests were made with flap track fairings attached. Two wingtip configurations were investigated, the ballasted tip and winglet tip. The test angle-of-attack range varied as the model lift was limited roughly to equivalent -0.5 to +1.25 g load values (scaled 1 g load was 144 lbf). Aerodynamic and pressure data were acquired to detect any unusual aerodynamic behavior and for possible use in adjusting the unsteady aerodynamic terms employed in the flutter analysis.

No flutter or undamped oscillations were encountered in this search. Some sample aerodynamic results are presented in Figure 8 for the ballasted tip on both the clean wing and the wing with flap track fairings. Plotted are variations with q of the lift-curve slope and angle-of-attack at zero lift for Mach numbers of 0.60, 0.70, and 0.80. It can be seen that the lift-curve slope for each M decreases by about 10 percent for a q increase of roughly 100 psf; this is due to the increasing nose-down twist of the outboard wing and resulting tip aerodynamic washout. These results indicate that the aeroelastic deformation of wing had no extreme aerodynamic effect over the test range. The flap track fairings apparently had little effect on these data. It is of interest to note that, near the cruise q of 30 psf, the wing with the high-q transition strip (Fig. 8) had about a 4 to 12 percent higher lift curve slope than the wing with the low-q transition strip (Fig. 6 (a)).

VII. Flutter Analysis

Flutter analyses were conducted for each wingtip configuration on the clean wing and on the wing with the flap track fairings. The results for the clean wing configurations will not be presented herein but are reported in reference 14. The analyses were made for M = 0.6, 0.7, 0.8, and 0.9 using doublet lattice unsteady aerodynamic theory[12] as implemented in the FASTOP[17] computer programs. Wing and winglet interference effects were included in the analysis. The p-k[18] method of solution was used in the FASTOP program. The wing was represented by an aerodynamic grid of 11 spanwise panels with 7 chordwise strips in each panel; the winglet was represented by 4 spanwise panels with 4 chordwise strips in each panel. The analyses of the wing with flap track fairings employed the calculated frequencies and mode shapes. For the normal and ballasted tip configurations, the first 5 vibration modes were used; for the winglet configuration, the first 6 vibration modes were used. Ten density values were considered and the flutter q was determined at each M for a matched tunnel velocity.

The analytical results indicated that the nature of the flutter mechanism remained unchanged when the flap track fairings were added to the clean wing. The flutter instability results when the wing torsion mode drops in frequency to couple with the wing first bending mode.

VIII. Flutter Results

For the model with the flap track fairings, a flutter boundary for each wingtip configuration was measured. The flutter tests were conducted with the model in a lifting condition within a range equivalent to a 0.35 to 0.70 g load, with most of the flutter points obtained at the higher values in that range. The model was destroyed during flutter of the normal-tip configuration at M = 0.71.

The experimental and analytical flutter results are presented in Figure 9. (The flow velocity (V) in fps at the test points can be computed from the relationship V = 510 x M.) The experimental flutter boundaries drawn for these configurations are based on the observed model activity at the low-damping as well as the actual flutter points. The boundaries exhibit the usual transonic dip with the minimum flutter q occurring near M = 0.82. The flutter modes of the three wingtip configurations were similar and of a conventional bending-torsion type. The flutter frequencies varied from 20 to 14 Hz.

The analyses predicted the experimental flutter q levels and Mach number trends very well for all three tip configurations. The doublet lattice unsteady aerodynamic theory used in the flutter analyses would not be expected to predict the flutter q recovery (increase) evident in the experimental data above M = 0.82.

The effect of the winglet on the wing flutter speed is shown more clearly in Figure 10. This figure presents the experimental flutter boundaries in terms of a normalized equivalent air speed at flutter, i.e., V_F/V_{REF} = (flutter q/reference q)$^{1/2}$. At Mach numbers from 0.7 to 0.8, the addition of the winglet reduced the flutter speed of the wing by an average of 7 percent whereas the addition of a mass-inertial representation of the winglet (the ballasted tip) reduced the wing flutter speed by an average of about 5 percent. Thus, most of the winglet effect on the wing flutter speed was due to the winglet mass, not aerodynamics.

IX. Summary of Results

An analytical and experimental study was made to determine the effect of a winglet on the flutter characteristics of a supercritical wing model representative of an executive-jet-transport wing. Aerodynamic and flutter tests were conducted at Mach numbers (M) from 0.6 to 0.95 on the model with a normal wingtip, a tip with winglet, and a normal shaped tip ballasted to simulate the winglet mass properties. For each wingtip configuration, a transonic flutter boundary was measured for the wing to which had been added ballasted flap track fairings to reduce the flutter dynamic pressures to reasonably low levels. The significant results from this study are:

1. The present flutter model was aerodynamically representative of the airplane supercritical wing both with and without winglet.

2. The flutter speed boundary measured for each wingtip configuration had roughly the same typical transonic shape with a minimum flutter speed occurring near M = 0.82. The compressibility drag break for this wing with/without winglet also occurred near this M, although the lift-curve slopes were still increasing up to M = 0.85.

3. At M = 0.7 to .8, the addition of the winglet and tip ballast reduced the wing flutter speed by about 7 and 5 percent, respectively. Hence, the winglet effect on flutter was more a mass effect than an aerodynamic effect.

4. The experimental flutter boundaries were predicted very well up to M = 0.82 by the flutter analyses which employed doublet lattice unsteady aerodynamics (with wing-winglet interference effects included). This subsonic theory cannot predict the flutter speed recovery that occurred beyond this M.

5. Static pressure distributions at the high dynamic pressure (q) levels at which flutter occurs are considerably distorted from those at the design cruise (relatively low-q) condition. The Jameson full potential transonic aerodynamic code yielded pressure distributions that agreed well with model test data for the single instrumented chord at M = 0.82 for both a low-q and high-q test condition.

X. References

[1]Whitcomb, Richard T., "Review of NASA Supercritical Airfoils," ICAS Paper No. 74-10, August 1974.

[2]Bartlett, Dennis W.; and Patterson, James C., Jr., "NASA Supercritical Wing Technology," NASA TM-78731, 1978.

[3]Whitcomb, Richard T., "Design Approach and Selected Wind-Tunnel Results at High Subsonic Speeds for Wing-Tip Mounted Winglets," NASA TN D-8260, 1976.

[4]Flechner, Stuart G.; and Jacobs, Peter F., "Experimental Results of Winglets on First, Second, and Third Generation Jet Transports," NASA TM-72674, 1978.

[5]McGrew, J. A.; Giesing, J. P.; Pearson, R. M.; Zuhuruddin, K.; Schmidt, M. E.; Kalman, T. P., "Supercritical Wing Flutter," AFFDL-TR-78-37, Final Technical Report, March 1978.

[6]Farmer, Moses G.; Hanson, Perry W.; and Wynne, Eleanor C., "Comparison of Supercritical and Conventional Wing Flutter Characteristics," NASA TM X-72837, 1976. (Also available in the Proceedings of AIAA/ASME/SAE 17th Structures, Structural Dynamics, and Materials Conference, May 1976).

[7]Yates, E. C., Jr.; Wynne, E. C.; Farmer, Moses G.; and Desmarais, R. N., "Prediction of Transonic Flutter for a Supercritical Wing by Modified Strip Analysis and Comparison with Experiment," NASA TM-83126, May 1981. (Available in Proceedings of AIAA Dynamic Specialists Conference, Atlanta, GA, April 9-10, 1981).

[8]Doggett, Robert V., Jr.; and Farmer, Moses G., "Preliminary Study of Effects of Winglets on Wing Flutter," NASA TM X-3433, 1976.

[9]Staff of Boeing Commercial Airplane Company, "Conceptual Studies of Wing Tip Extensions, Winglets, and Wing Load Alleviation for the Boeing 747 Energy Efficient Transport," NASA CR-3164. Final Report, May 1977-May 1979.

[10]Staff of Boeing Commercial Airplane Company, "Selected Advanced Aerodynamic and Active Controls Technology Concepts Development on a Derivative B-747 Aircraft," NASA CR-3295, June 1980.

[11]Kehoe, M. W., "KC-135A Winglet Flight Flutter Test Program," AFFTC-TR-81-4, June 1981.

[12]Kalman, T. P.; Rodden, W. P.; and Giesing, J. P, "Application of the Doublet Lattice Method to Non-Planar Configurations in Subsonic Flow." J. Aircraft, Vol. 8, No. 6, June 1971, pp. 406-413.

[13]Chipman, R.; Waters, C.; MacKenzie, D., "Numerical Computation of Aeroelastically Corrected Transonic Loads," AIAA Paper No. 79-0766, presented at AIAA 10th SDM Conference, April 1979.

[14]Rauch, F. J., Jr.; and Waters, C., "Analyses and Initial Tests Conducted on a 1/6.5-Size Flutter Model of an Executive-Jet-Transport Supercritical Wing With and Without Winglet," NASA CR-165857, Nov. 1978.

[15]Jarvis, Robert, "Wind-Tunnel Model Deflections System," Paper presented at Instrumentation Society of America 25th International Instrumentation Symposium, Anaheim, California, May 1979.

[16]Cole, Patricia H., "Wind Tunnel Real-Time Data Acquisition System," NASA TM-80081, 1979.

[17]Many authors, "An Automated Procedure for Flutter And Strength Analysis and Optimization of Aerospace Vehicles (FASTOP)," Vol. 1, pp. 95-98, AFFDL-TR-75-137, 1975.

[18]Hassig, Hermann J., "An Approximate True Damping Solution of the Flutter Equation by Determinant Iteration," J. Aircraft, Vol. 8, No. 11, Nov. 1971, pp. 885-889.

Table I. Measured Wingtip Mass Properties

Wingtip	Wingtip span	Mass	c.g. location		Inertia about c.g.		
			x**	y**	Pitch, I_{yy}	Roll, I_{xx}	Yaw, I_{zz}
	in.	lbm	in.	in.	lbm-in.^{2}	lbm-in.^{2}	lbm-in^2
Normal*	3.070	0.2575	55.14	77.75	2.45	0.28	2.62
Winglet*	3.070	.4918	56.91	79.01	10.35	4.94	7.88
Ballasted*	3.070	.4916	56.80	77.80	10.117	.81	10.315

*Does not include structural attachment tabs which extend outboard from main wing and overlap the wingtip panel.

**Coordinates: x-streamwise, y-spanwise, z-vertical. Origin is intersection of wing leading-edge extension with airplane centerline.

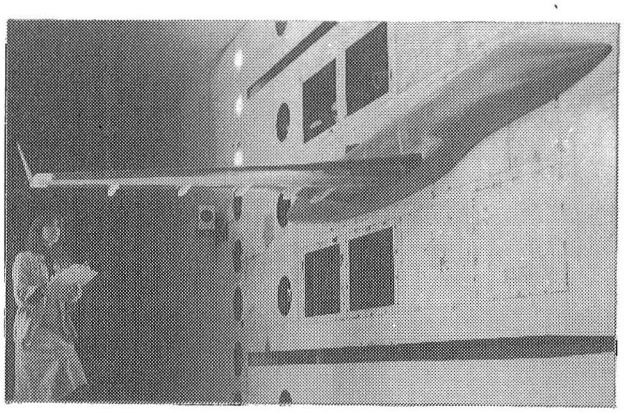

Fig. 1 Model with winglet and flap track fairings mounted in wind tunnel.

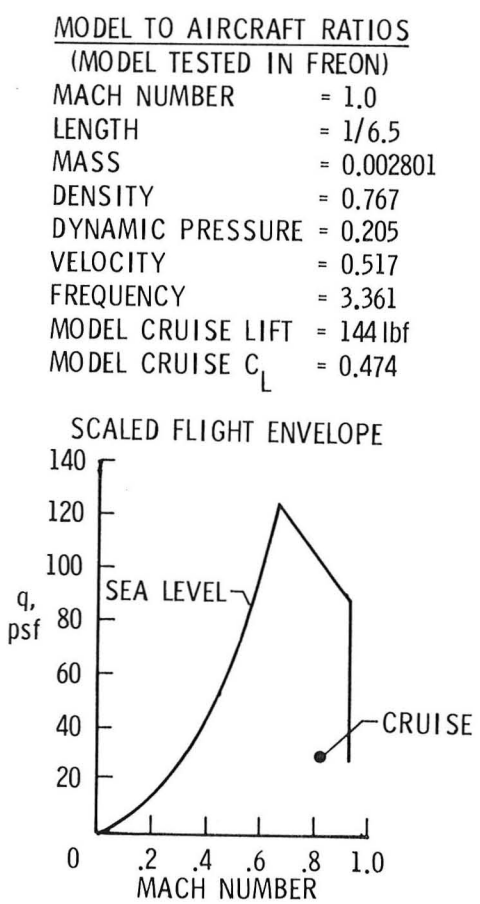

Fig. 2 Scaling ratios and scaled flight envelope for clean-wing model.

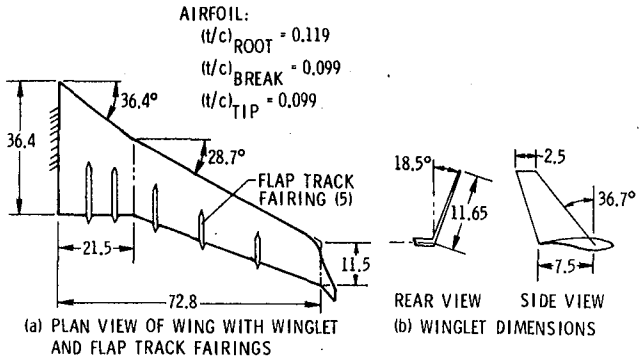

Fig. 3 Model geometries. Dimensions are in inches or degrees.

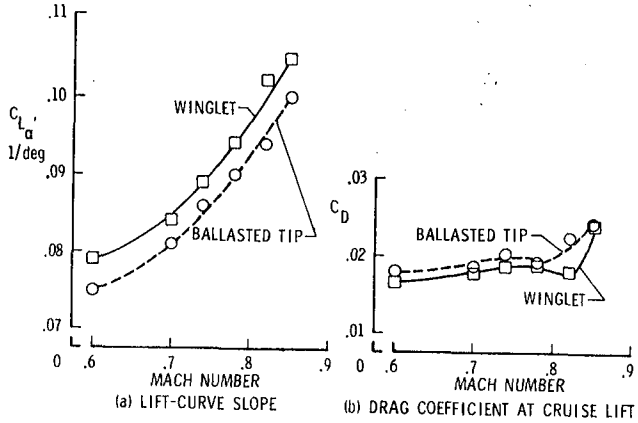

Fig. 6 Aerodynamic data measured on clean wing at cruise dynamic pressure.

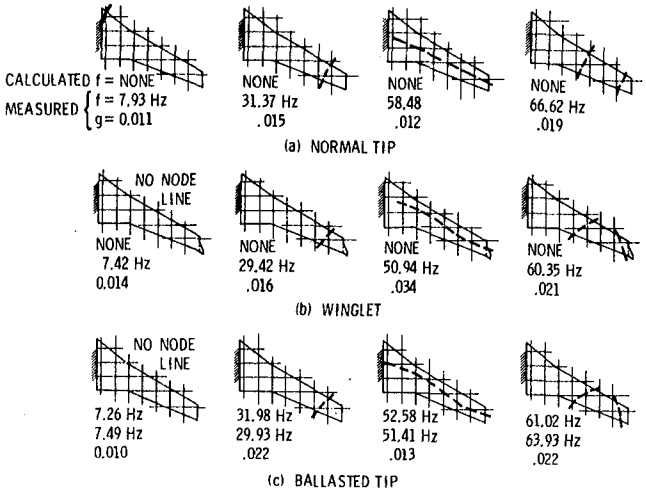

Fig. 4 Vibration characteristics of clean wing.

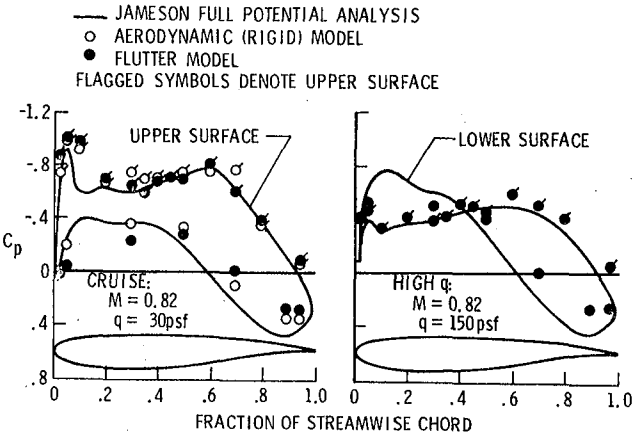

Fig. 7 Static pressure distributions at 0.30 semispan for cruise C_L.

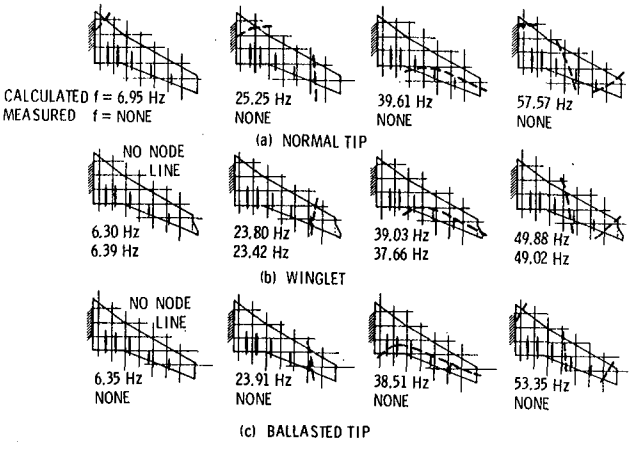

Fig. 5 Vibration characteristics of wing with flap track fairings.

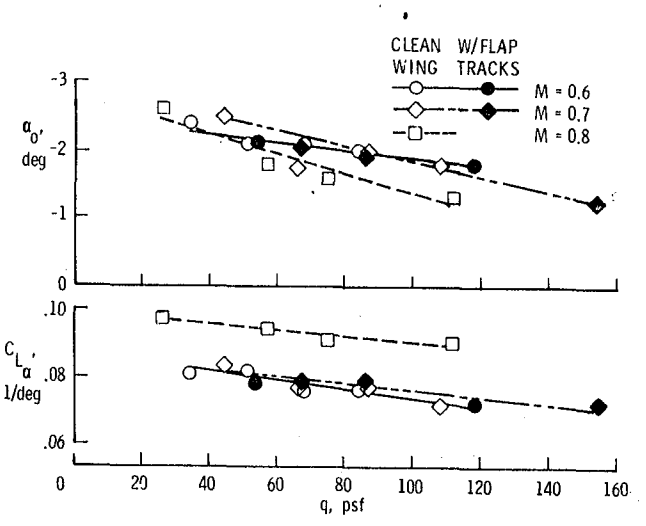

Fig. 8 Measured effects of elastic deformation on C_{L_α} and α_o.

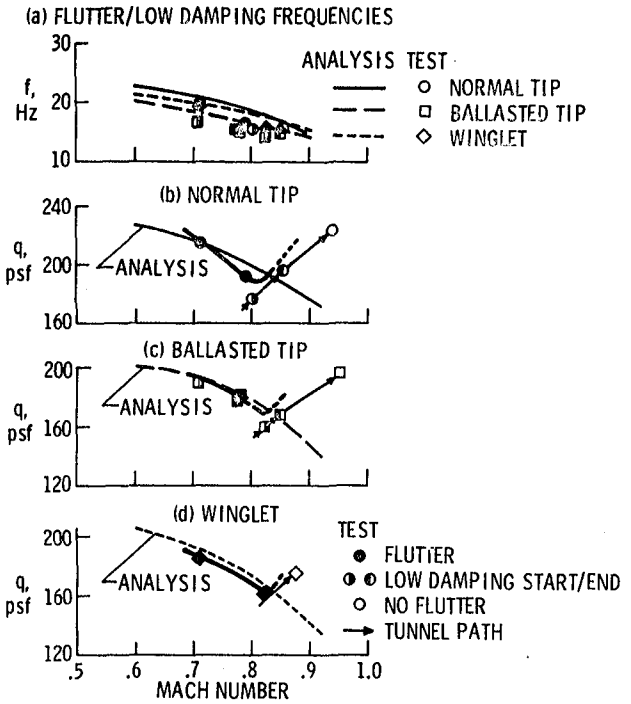

Fig. 9 Flutter test and analysis results.

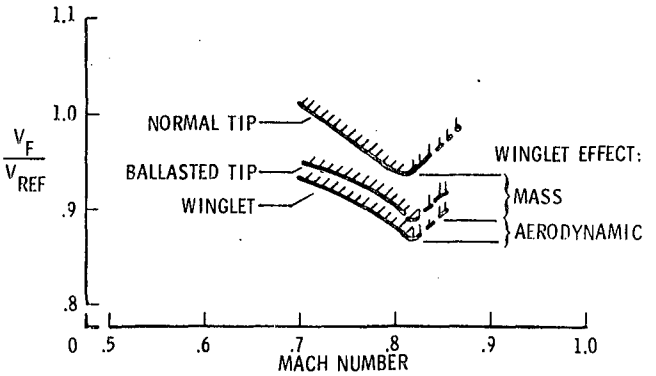

Fig. 10 Winglet effect on wing flutter speed.

1. Report No.	2. Government Accession No.	3. Recipient's Catalog No.
NASA TM-83279		

4. Title and Subtitle	5. Report Date
TRANSONIC FLUTTER STUDY OF A WIND-TUNNEL MODEL OF A SUPERCRITICAL WING WITH/WITHOUT WINGLET	March 1982
	6. Performing Organization Code 505-33-53-01
7. Author(s) Charles L. Ruhlin, Frank J. Rauch, Jr.,* and Catherine Waters*	8. Performing Organization Report No.
	10. Work Unit No.
9. Performing Organization Name and Address NASA Langley Research Center Hampton, VA 23665	11. Contract or Grant No.
	13. Type of Report and Period Covered Technical Memorandum
12. Sponsoring Agency Name and Address National Aeronautics and Space Administration Washington, DC 20545	14. Sponsoring Agency Code

15. Supplementary Notes

*Grumman Aerospace Corporation
Bethpage, NY 11714

This paper was presented at the 23rd AIAA/ASME/ASCE/AHS Structures, Structural Dynamics and Materials Conference, May 10-12, 1982, New Orleans, LA

16. Abstract

The scaled flutter model was a 1/6.5-size, semispan version of a supercritical wing (SCW) proposed for an executive-jet-transport airplane. The model was tested cantilever-mounted in the Langley Transonic Dynamics Tunnel with a normal wingtip, a wingtip with winglet, and a normal wingtip ballasted to simulate the winglet mass properties. Flutter and aerodynamic data were acquired at Mach numbers (M) from 0.6 to 0.95. The measured transonic flutter speed boundary for each wingtip configuration had roughly the same shape with a minimum flutter speed near M = 0.82. The winglet addition and wingtip mass ballast decreased the wing flutter speed by about 7 and 5 percent, respectively; thus, the winglet effect on flutter was more a mass effect than an aerodynamic effect. Flutter characteristics calculated using a doublet-lattice analysis (which included interference effects) were in good agreement with the experimental results up to M = 0.82. Comparisons of measured static aerodynamic data with predicted data indicated that the model was aerodynamically representative of the airplane SCW.

17. Key Words (Suggested by Author(s))		18. Distribution Statement
Flutter Supercritical Wing Winglet Aeroelasticity	Wind-tunnel Test Transonic Effects	Unclassified - Unlimited Subject Category - 05

19. Security Classif. (of this report)	20. Security Classif. (of this page)	21. No. of Pages	22. Price
Unclassified	Unclassified	10	A01

For sale by the National Technical Information Service, Springfield, Virginia 22161